CT of Cardiac Function and Wall Motion

35

Prabhakar Rajiah and Suhny Abbara

Functional evaluation is an important component of cardiovascular imaging, contributing to diagnosis, risk stratification, prognosis, determining optimal therapy, and follow-up after treatment. For example, left ventricular (LV) function is an important predictor of survival in patients following myocardial infarction [1] and CABG surgery [2] as well as other nonischemic cardiomyopathies. Right ventricular (RV) function is a prognostic determinant in conditions such as acute pulmonary embolism (PE), congenital heart disease (CHD), and arrhythmogenic right ventricular dysplasia (ARVD). Left atrial function is a predictor of recurrence of atrial fibrillation after pulmonary vein ablation. Although cardiac CT is primarily utilized in the evaluation of coronary arteries, it is also a valuable tool in the evaluation of cardiac function as well, particularly when echocardiography is not adequate and cardiovascular magnetic resonance (CMR) is contraindicated or associated with significant artifacts.

In this chapter, we review the role and technique of CT in the evaluation of ventricular and atrial function.

Imaging of Cardiac Function

There are several imaging modalities available for the evaluation of ventricular and atrial function, including echocardiography, magnetic resonance imaging (MRI), nuclear medicine, and angiography. *Echocardiography* is the most commonly used modality for the evaluation of cardiac function. It is widely available, inexpensive, portable, can be performed in hemodynamically unstable patients at bedside, does not have radiation, and there are no major contraindications. However, echocardiography is operator dependent and may be limited by acoustic windows, especially in patients with obesity, COPD, chest wall deformities, and surgeries, particularly in the evaluation of RV. It also relies on geometrical assumptions, which make evaluation of remodeled and complex hearts challenging. There is also poor contrast between blood and myocardium, as a result of which it has lower accuracy and reproducibility [3]. While LV volume is obtained by Simpson's rule, mass is evaluated in M-mode. Transesophageal echocardiography (TEE) has improved acoustic window, but there are associated complications of an invasive procedure and general anesthesia. New techniques such as 3D result in improved quantification, with higher accuracy and reproducibility [3], but add to the time and are prone to artifacts.

CMR has several advantages including good spatial and temporal resolutions, high contrast between blood and myocardium which allows accurate delineation of the endocardial contour, no radiation, and no geometrical assumptions. It can perform both qualitative and quantitative evaluation of global and regional systolic function, with possibilities of diastolic functional evaluation as well. CMR has been shown to be the gold standard in quantification of ventricular function, due to high accuracy and reproducibility [4]. Quantification is usually performed in short-axis view utilizing modified Simpson's method. Cine images in other planes including two, three, and four chamber are used to evaluate regional wall motion abnormalities. CMR also allows for anatomical evaluation and tissue characterization in the same study. However, CMR is contraindicated in patients with several intracardiac devices as well as claustrophobic patients. CMR is also not widely available, is expensive, requires higher technical expertise, takes longer time, and is challenging in patients with arrhythmia or those unable to lay flat. In children, intubation and anesthesia are often required.

Nuclear medicine techniques for quantification of LV function include gated radionuclide ventriculography (RVG), ECG-gated single-photon emission computed tomography (SPECT), and positron emission tomography (PET). With

P. Rajiah · S. Abbara (✉)
Department of Radiology, Cardiothoracic Imaging Division, UT Southwestern Medical Center, Dallas, TX, USA
Suhny.Abbara@utsouthwestern.edu

U. J. Schoepf (ed.), *CT of the Heart*, Contemporary Medical Imaging, https://doi.org/10.1007/978-1-60327-237-7_35

RVG or MUGA (multiple-gated acquisition), patient's RBCs are labelled, and ECG-gated cardiac scintigraphy is obtained over several heartbeats to generate a single composite cardiac cycle. This can quantify global and regional function and volumes, both at rest and stress. The advantage of this technique is that it does not rely on geometrical assumptions [5]. Disadvantages include lower temporal and spatial resolution and limited accuracy in arrhythmias. There are long preparation and examination times. Function can also be obtained from a gated SPECT utilized for myocardial perfusion imaging, by analyzing the ventricular contours [6], which correlates well with CMR [7]. Regional EF with handgrip has been shown to be highly sensitive and specific for coronary artery disease [8]. Disadvantages of SPECT include lower spatial resolution, inaccuracy in ischemia/infarct due to lower uptake in subendocardial region [9], and decreased accuracy in attenuation artifacts as well as patients with small or large hearts [3]. Variability has been noted with Tl-201 scans and between different software algorithms [3]. Repeated radionuclide injections and radiation dose are additional concerns. Similarly, function can be obtained from ECG-gated PET performed for myocardial perfusion and metabolism imaging, which correlates well with CMR [6]. PET has higher spatial resolution than SPECT but has lower temporal resolution than CMR, which results in underestimation of function. Due to inclusion of papillary muscles with myocardial wall, the volumes are lower than CMR [6]. Radiation is a concern with all the nuclear medicine techniques.

Cine ventriculography with catheter angiography is not routinely used for quantification of ventricular function. It is an invasive procedure, requires contrast, uses radiation, has geometric assumptions and restrictions from projection images. It is limited in evaluation of some regions, especially in complex, irregular shapes, and has significant variability in regional wall motion assessment due to variable cardiac rotation and lack of reliable landmarks [3].

Computed Tomography

Advantages and Disadvantages

CT scan has several advantages in the evaluation of ventricular function such as high isotropic spatial resolution, good temporal resolution, high contrast between ventricular lumen and myocardium, and multi-planar reconstruction capabilities. CT quantification does not rely on geometric assumptions. Additional information can be obtained on the morphology of the heart as well as coronary arteries and any adjacent structure. CT is not operator dependent, is widely available, and has rapid turnaround time, making it suitable for patients who cannot lay still for prolonged periods of time. For functional evaluation, CT is typically utilized when MRI is contraindicated or suboptimal due to artifacts or if echocardiography does not provide adequate information due to poor acoustic window, especially for right ventricle. Common contraindications for MRI include metallic objects in the eye, older versions of intracardiac devices (pacemakers, defibrillators), claustrophobia, and inability to lay flat for prolonged period. CT for functional evaluation has been considered an appropriate indication in the 2010 ACCF guidelines [10]. Disadvantages of CT include the use of ionizing radiation which is associated with several theoretical risks and the use of contrast media in patients with renal dysfunction which is associated with nephrotoxicity. Premedication is required for patients with history of contrast allergy. Image quality is compromised in patients with severe arrhythmias, with poor definition of borders, and with potential increases of radiation dose in some scanners due to the opening of image acquisition window.

Scan Mode

Cardiac cycle starts with isovolumetric contraction at the end of ventricular filling, followed sequentially by ventricular systole, isovolumic ventricular relaxation, and then diastole. To capture the cardiac volumes and function, ECG gating and high temporal resolution are required to essentially freeze the cardiac motion without any motion artifacts. Since multiple cardiac phases are required in the R-R interval, particularly end-systole (ES) and end-diastole (ED), retrospective ECG gating is required. The heart is scanned in the spiral mode, with the table continuously moving through the gantry, and images are acquired throughout the cardiac cycle, over multiple heartbeats. ECG tracing is also simultaneously acquired, and images are retrospectively reconstructed. A low pitch (<1.0), dependent on the heart rate, is utilized to image the heart throughout R-R interval with areas of oversampling. Due to this, there is an overlap of the same anatomy at different R-R intervals, which can be used for multisegment reconstruction. High spatial and temporal resolutions are required for accurate quantification. The highest possible spatial resolution should be selected to accurately delineate the endocardial borders and minimize partial volume averaging at the blood pool-myocardium interface which can be seen at the apex [3].

High temporal resolution is required to achieve artifact-free images of the myocardial contraction. A temporal resolution of 100–250 milliseconds (ms) is recommended for the evaluation of systole and diastole and higher if resolu-

tion of rapid ventricular filling and ejection phase is recommended. 80–90 milliseconds has been suggested for adequate evaluation of wall motion in CMR [3, 11], but 19.1 ms or less is necessary to avoid motion artifacts [12], especially in the posterior LV wall [11]. The temporal resolution of a scanner is determined primarily by the gantry rotation time. Since only a partial scan reconstruction algorithm is used, effective temporal resolution is the time taken to rotate the tube 180 plus fan angle. In the earlier scanners with few detectors, the gantry rotation time was long, with limited temporal resolution, as a result of which, the EDV can be underestimated and ESV can be overestimated since the position of ventricles at EDV and ESV is averaged over multiple heartbeats. However, improvements in scanner technology over the last decade have resulted in shorter gantry rotation times and improved temporal resolution. This is further improved in dual-source scanners, where the temporal resolution is one fourth of the gantry rotation time, resulting in effective temporal resolution of up to 75 milliseconds. Another option to improve temporal resolution in a spiral acquisition is to use multi-segment reconstruction, i.e., reconstruct data from same phase of cardiac cycle in consecutive heartbeats. The temporal resolution is equal to gantry rotation time divided by 2*n*, with n being the number of segments. The higher the number of segments, the higher will be the temporal resolution. However, this requires a steady heart rate; otherwise there will be beat to beat variation of the position of the heart resulting in artifacts. Even with steady heartbeat, the heart may not be in the same location due to complex cardiac contraction. Multi-segment reconstruction may also require reduction of spiral pitch, which will increase scan time and thus radiation dose. Motion artifacts can be eliminated by using wide-array or volume scanners with z-coverage up to 16 cm or dual-source scanners with high pitch (up to 3.4), as a result of which the entire heart can be scanned in one heartbeat.

Medications and Contrast

Beta-blockers are routinely used in coronary CTA to reduce the heart rate and minimize coronary artery motion, but this is not required for evaluation of cardiac function. In addition, studies have shown there is a small but not negligible reduction in LV function after administration of propranolol in healthy subjects [13, 14] as well as those with heart disease [15, 16], due to negative inotropic action and increased ESV.

Contrast injection should be optimized depending on the chamber of interest. If both ventricles are being evaluated, a triphasic injection protocol is used to adequately opacify both the ventricles. With adequate contrast opacification of RV, i.e., >176 HU, the volume measurements are more comparable with CMR [17]. In the first phase, a full dose of contrast is administered at a rate of 4–7 ml/s to opacify the left ventricle. In the second phase, either a slower injection of contrast at 2–4 ml/s or a contrast saline admixture (50:50, 60:40, or 70:30) at the same rate of 4–7 ml/s is injected to opacify the right ventricle. In the final phase, saline flush is injected at 5–7 ml/s to eliminate the streak artifacts in SVC and the right atrium. Scan acquisition is triggered either by using a bolus tracking technique, with the ROI placed in the descending aorta, or a timing bolus technique following injection of a small bolus of contrast first, although this takes additional time and also wastes some amount of contrast [18]. Bolus tracking has been shown to provide more homogeneous enhancement [19]. Scanning is typically 4–6 s after peak aortic opacification [20].

Radiation Dose Reduction Strategies

With retrospective ECG gating, the radiation dose is significantly high since data is obtained throughout the cardiac cycle (Fig. 35.1), with values from 14.8 to 21.1 mSv [21]. However, the radiation dose can be reduced by using ECG-based tube current modulation, where the peak tube current is delivered only in specific cardiac phase(s), i.e., ED and ES, and ramped down to 4–20% of peak tube current for the rest of the R-R interval (Fig. 35.2). This technique has been shown to allow radiation dose savings of up to 60% [22, 23]. A prospective ECG-triggering mode, where data is acquired only in one portion of the cardiac cycle, is not useful for estimation of function. However, prospective ECG gating with wider padding can be utilized to evaluate cardiac function, although this does not provide any significant radiation dose savings compared to retrospective ECG gating [24]. Another technique is a prospectively ECG-triggered dual-step pulsing protocol in a dual-source scanner, in which a prospectively ECG-triggered window is obtained at low radiation dose (20% tube current) across a selected portion of cardiac cycle (10–90%), with a full tube current only in a selective portion of cardiac cycle (65–75% RR). X-ray tube is also turned off in between heartbeats. This provides both functional data at lower radiation dose as well as normal radiation dose data for detailed evaluation of coronary arteries. This provides accurate quantification compared to CMR with lower radiation dose (6.2 + 1.8 mSv) [21]. Other radiation dose reduction strategies can also be applied for functional evaluation, including lowering tube voltage, lowering tube current, automatic tube current modulation techniques, and iterative reconstruction algorithms.

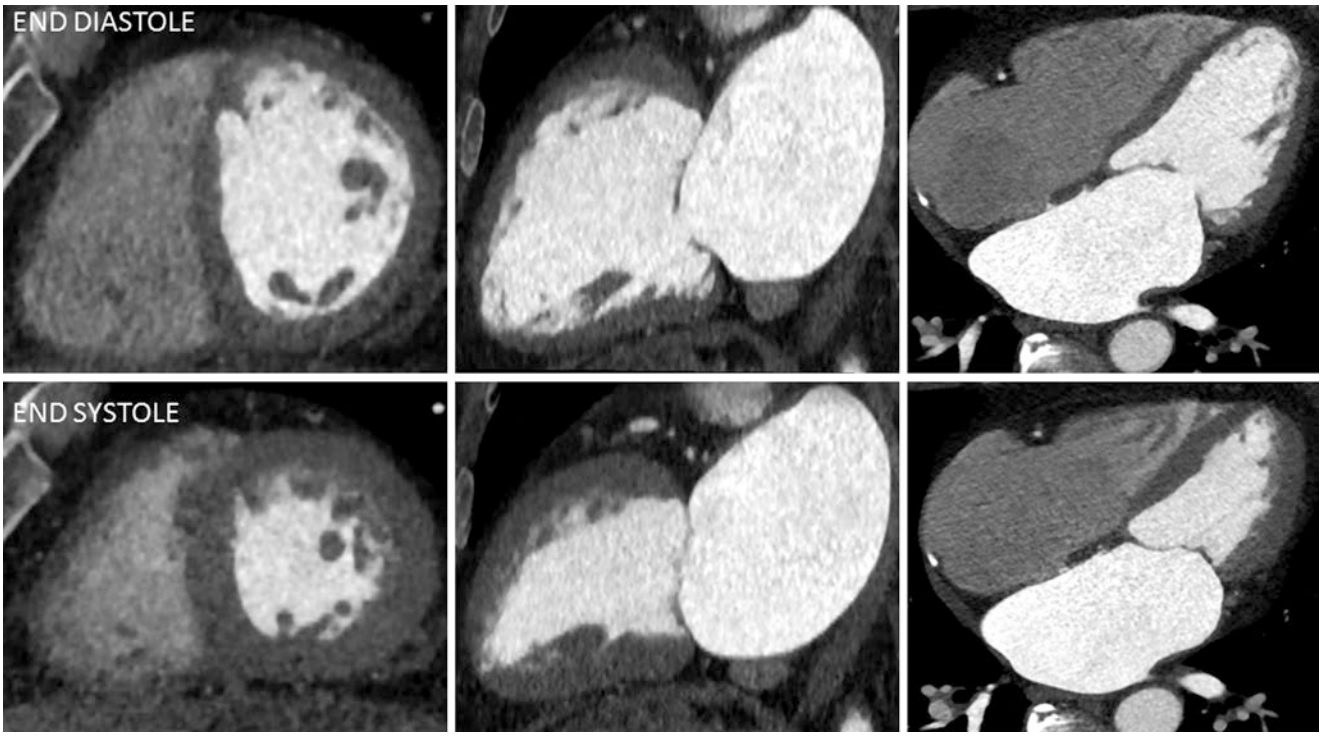

Fig. 35.1 Retrospective ECG gating without ECG-based tube current modulation. Short-axis (left), two-chamber (middle), and four-chamber (right) reconstructions of the heart at end-diastole (top row) and end-systole (bottom row). Since full tube current is delivered throughout the cardiac cycle, there is no significant difference in image quality between the two sets of images, albeit a high radiation dose

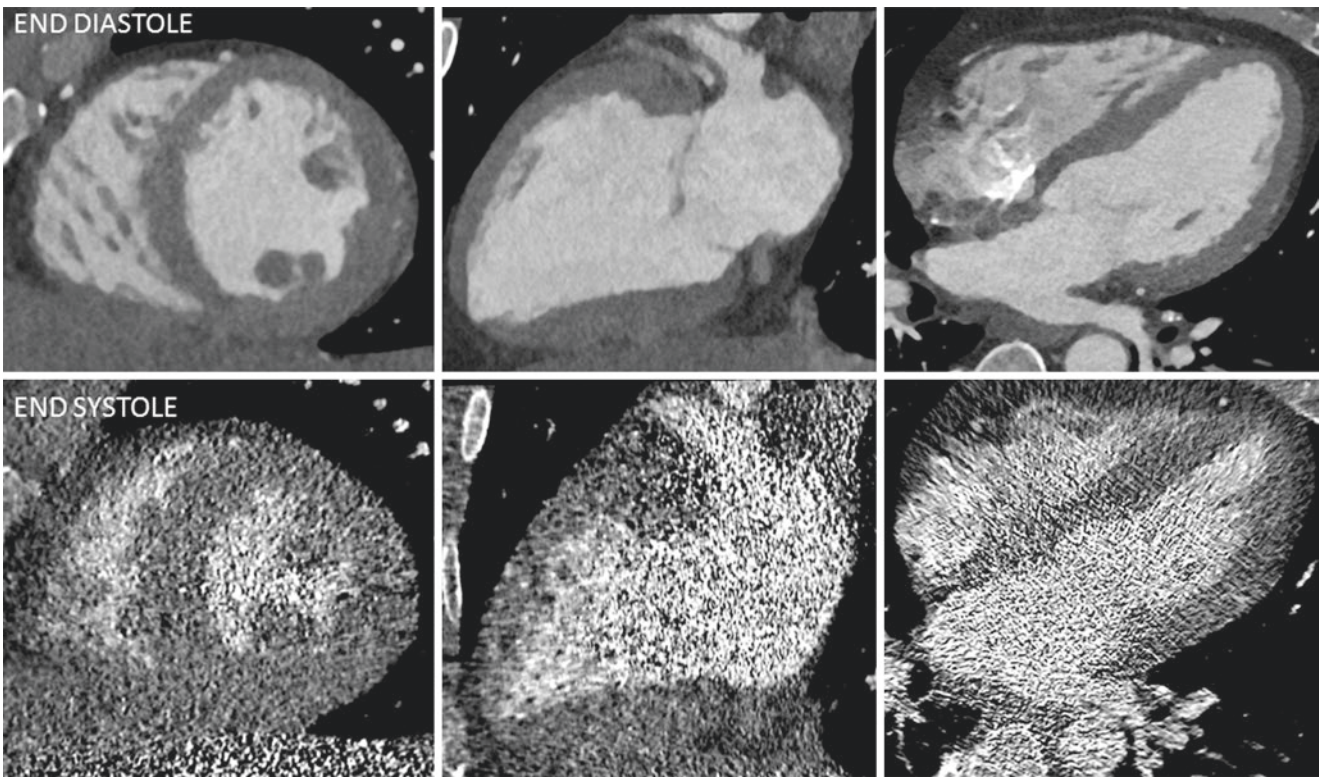

Fig. 35.2 Retrospective ECG gating with ECG-based tube current modulation. Short-axis (left), two-chamber (middle), and four-chamber (right) reconstructions of the heart at end-diastole (top row) and end-systole (bottom row). Note the higher noise seen in the end-systolic images since these images are obtained at 20% of maximum tube current. In spite of the higher noise at end-systole, these images are adequate for delineation of endocardial and epicardial contours for functional, volume, and mass measurements

Image Reconstruction

After acquisition of data, images are constructed at 5–10% increments throughout the R-R interval, generating either 10 or 20 cardiac phases. In a single-source scanner, no advantage is gained by using 20 instead of 10 phases, but there is an increase in reconstruction time and space taken for storing these images. In dual-source scanners with good temporal resolution, the full benefit of good temporal resolution may be gained by using 20 phases [20]. No significant difference in EF and volumes was noted between 10 and 20 phases, both for single-source [25] and dual-source scanners [26]. Images can be displayed as 2D cine loops, and most workstations allow manipulation of the planes in any direction. Typically short-axis, two-chamber, three-chamber, and four-chamber planes are used for qualitative global and regional functional evaluation. Thin slices are not mandatory for evaluation of function, with 1.5, 2.0, or 2.5 mm slices with no overlap of intervals of 1 or 1.5 mm commonly used. Noise reduction strategies, including iterative reconstruction, increase the CNR and hence improve the correlation of ventricular volumes, mass, and function with CMR [27].

Post Processing

Quantitation of the volumes and function can be performed using either manual, semiautomatic, or fully automatic techniques.

(a) *Area-length method*. In this technique, volume of the left ventricle (V) is calculated from the area (A) and length (L) of the left ventricle, using the formula $V = \frac{8}{3} \times \frac{A^2}{\pi L}$.

This is measured in one of the long-axis views (vertical or horizontal). The length is measured from mitral annulus to the apex, and the area is measured in the same plane. This technique uses geometrical assumptions to measure the volume, i.e., assuming an ellipsoid shape.

(b) *Biplane area-length method*. In this variation of the area-length product, both the vertical and horizontal long axes are used to calculate the volume. This method also relies on geometrical assumptions.

(c) *Simpson's method*. In Simpson's method, the volumes are determined by summing up areas of LV cavity at each short-axis slice and multiplying it with slice thickness, using the formula volume $\sum A_N \times S$, where A is the cross-sectional area and S is the section thickness. Multiple parallel short-axis slices are utilized. Endocardial contours are drawn, either manually, automatically, or semiautomatically, both at end-diastole and end-systole in all the slices along the entire length of ventricle (Fig. 35.3). Although the LV limits can be automatically determined using the software, determination of the most basal and apical slices can be challenging. The most basal slice is just forward to the atrioventricular ring and has myocardium in at least 50% of its perimeter. The most apical slice is the last image with contrast-opacified lumen. Determination of the correct ED and ES phase can also be done manually, semiautomatically, or automatically. End-diastole is defined as QRS onset, which corresponds to the phase with the largest cardiac dimension and following mitral valve closure. End-systole is the phase where the cardiac dimension is the smallest and precedes mitral valve opening. Papillary muscles are included in the ventricular lumen. For evaluation of myocardial volume, epicardial contours are drawn in end-diastolic phase, and the mass is calculated by using the formula $\sum A_N \times S$ x $\acute{\rho}$, where $\acute{\rho}$ is the myocardial density (1.05 g/cm3). This three-dimensional technique is considered accurate since it does not rely on geometric assumptions. It has been shown superior to the area-length technique, which overestimates EDV, ESV, and SV [28] and agrees more with 2D echo, MRI, CVG, and gated SPECT. Sources of errors include inappropriate plane, selecting basal and apical slices, selecting ED and ES phases, and drawing endocardial and epicardial borders. Manual contouring, even with semiautomatic software, is time-consuming, subjective, and observer dependent. Semiautomatic and automatic techniques significantly shorten the processing time due to advanced software, automatic generation of cardiac views, automatic selection of ED and ES phases, and automatic segmentation. Automatic techniques also decrease interobserver variability without significant changes in volumes and function [29–31], although some studies showed differences in LVEDV [29].

Threshold-Based Segmentation

Threshold-based segmentation is an automatic technique that utilizes the differences in attenuation between the blood pool and myocardium. The mitral annular plane may have to be verified or defined manually since the contrast attenuation is similar in the atrium and ventricle,

following which the contrast-filled LV is automatically segmented in all the phases. Ventricular volume is calculated by summing all the contiguous voxels whose attenuation is above that of a predefined threshold (Fig. 35.4). Although volumes are typically calculated from short-axis view in 2D, recent software also allow 3D volume quantification. Segmented pixels are displayed in color. If the segmentation does not look accurate, the attenuation threshold can be altered to make the color fit the cavity. In most softwares, the LV function automation works readily, while RV function requires some kind of manual correction. Time-volume curves can be generated since all the phases are segmented. This technique requires good opacification of the blood pool with contrast, with at least 150–200 HU attenuation difference between myocardium and blood pool. Errors will be seen if there is high attenuation material such as dense contrast in veins or right heart or pacemaker leads, which may lead to inclusion of RA or RV in LV blood pool. Similar errors can also emanate from unbroken column of contrast in VSD [30, 32]. In this technique, the papillary muscles are not included in the blood pool due to their different attenuation and hence do not contribute to the volume, as a result of which the EDV and ESV are smaller, with no change in EF [20]. Threshold-based technique has been shown to be accurate and reproducible with lower interobserver variability with shorter-processing time [3]. With manual contours, the papillary muscles are within the blood pool, and hence the volumes are larger, which correspond to MRI numbers due to similar measurement [33]. A study found differences of 5.6–30.1% for LV volumes, 5.8–9.4% for LV mass, and 4.3–6.0% for LV EF [34].

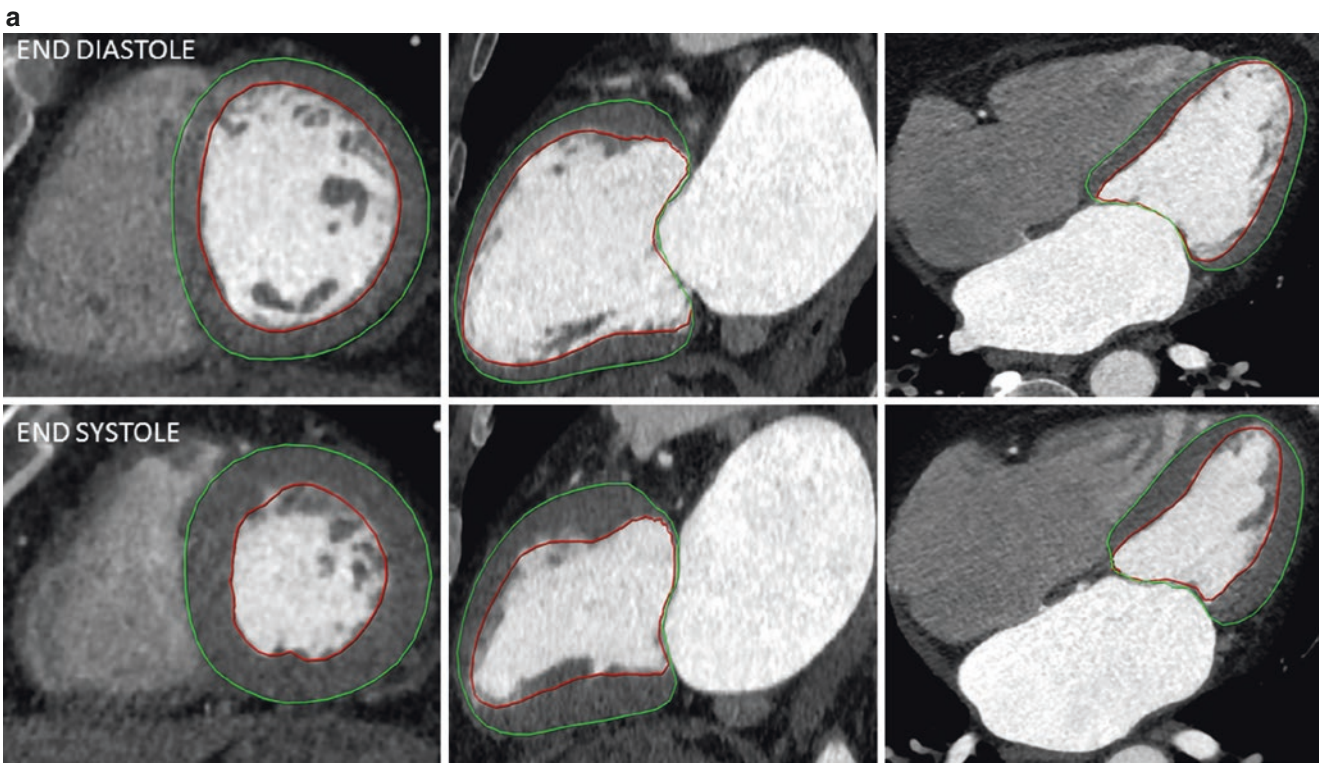

Fig. 35.3 Quantification of the left ventricle. (**a**) Values obtained from the above contours include ejection fraction, end-diastolic volume, end-systolic volume, stroke volume, cardiac output, and myocardial mass. All these can be indexed to the body surface area (BSA) (**b**) Short-axis (left), two-chamber (middle), and four-chamber (right) reconstructions of the heart at end-diastole (top row) and end-systole (bottom row). Endocardial (red) and epicardial (green) contours are drawn in the left ventricle, both in end-diastolic and end-systolic images.

b

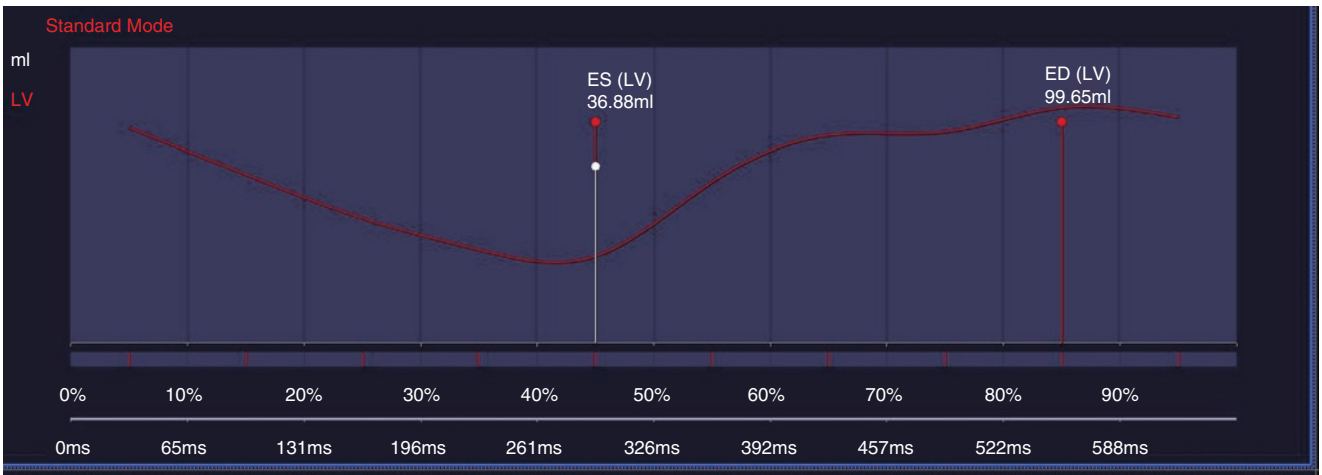

Standard Values | Indexed Values

Standard Mode		LV	Normal Values
Ejection Fraction	%	63	56 - 78
Myocardial Mass ED	g	96.82	75 - 175
Stroke Volume	ml	62.77	33 - 97
ED Volume	ml	99.55	58 - 154
ES Volume	ml	36.88	13 - 51
Cursor Volume	ml	36.88	
Cardiac output	(l/min)	5.71	2.65 - 5.98

Fig. 35. 3 (continued)

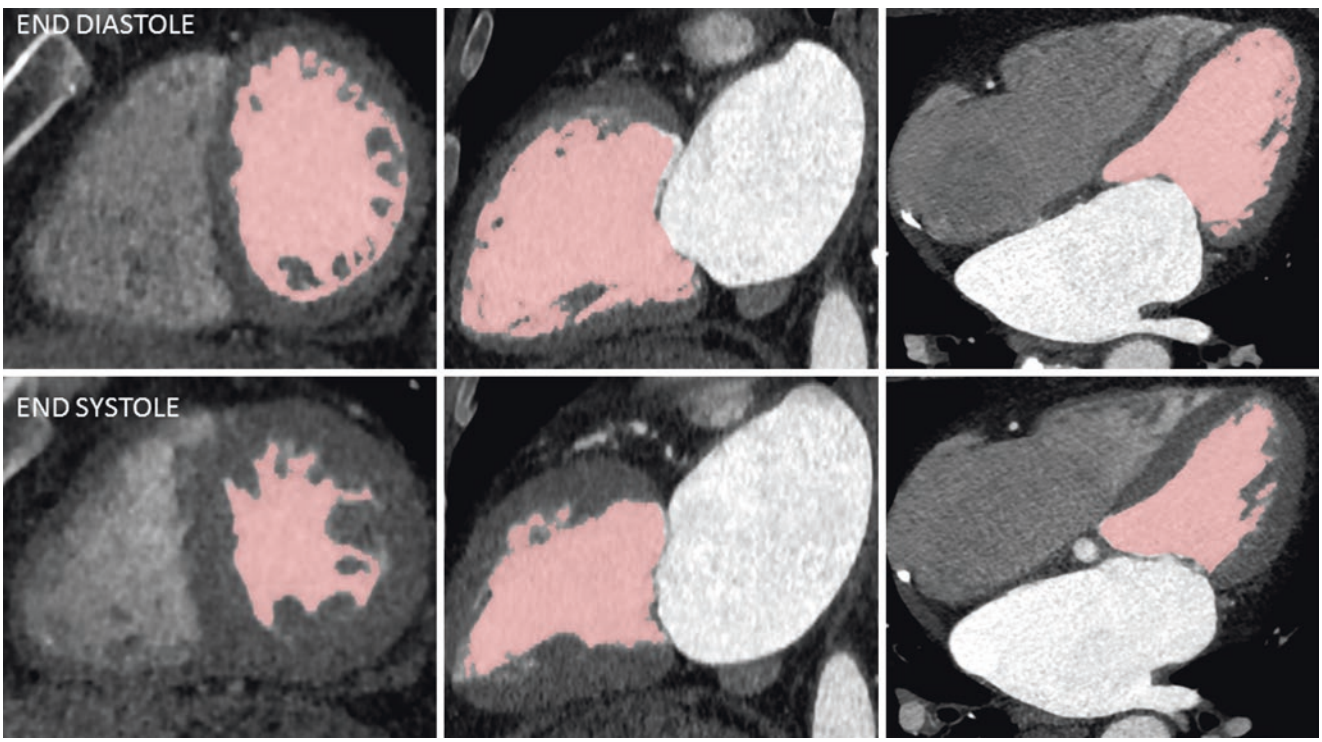

Fig. 35.4 Quantification using threshold segmentation. Short-axis (left), two-chamber (middle), and four-chamber (right) reconstructions of the heart at end-diastole (top row) and end-systole (bottom row). The threshold-based segmentation technique utilizes the differences in attenuation between contrast in the blood pool and the myocardium. All the contiguous voxels whose attenuation is above that of a predefined threshold are identified in pink. Ventricular volume is calculated by summing all these voxels

Interpretation of Results

Qualitative

Global function can be qualitatively evaluated in cine images at multiple planes. All the currently available softwares automatically generate the standard cardiac planes, typically a short-axis view and two long-axis views. Any other plane can also be generated by manual interaction. Global systolic function can be qualitatively classified as normal, reduced (mild, moderate, and severe), or hyperdynamic. Regional wall motion abnormalities can be evaluated using the 17-segment AHA model and multi-planar CT reconstructions, including short-axis, two-chamber, three-chamber, and four-chamber views. There are six basal, six mid, and four apical segments, accounting for 35%, 35%, and 30% of myocardial volume, respectively along with an apical cap. Regional wall motion can be classified as normal (inward motion in systole), hypokinesis (decreased wall motion), akinesis (no wall motion), and dyskinesis (paradoxical wall motion). Abnormalities have to be seen in two different views to be considered true positive.

Quantitative

Several quantitative parameters are derived from the post-processed images as above. Parameters of global systolic function include the *stroke volume*, which is the volume of blood ejected from the ventricle with each heartbeat, i.e., SV = EDV-ESV. This represents the blood ejected both forward and backward and hence includes regurgitant flow. The stroke volume of the right and left ventricles is the same, assuming there is no regurgitation or shunting. *Cardiac output (CO)*, the volume of blood pumped in 1 min, is SV × HR (ml/min). *Ejection fraction* is a percentage, which is SV/EDV × 100%. *Myocardial mass* is quantified as end-diastolic myocardial volume × density. Usually, a density of 1.05 g/cm3 is used. All these measurements can be indexed to the body surface area (BSA) to derive indexed values. If images are reconstructed in all cardiac phases, a time-volume curve can also be generated, which provides additional time-dependent variables such as peak ejection rate (PER), peak filling rate (PFR), time to PER, and time to PFR.

Regional wall motion can also be quantified using several indices if at least 8–10 cardiac phases are available. Normal LV ejection is a combination of radial wall thickening, circumferential shortening, and longitudinal shortening [11]. Parameters evaluated include *myocardial wall thickness*, which is calculated in orthogonal plane between endocardial and epicardial contour. Myocardium normally measures 6–8 mm in end-diastole and 10–14 mm in end-systole [35]. It is focally decreased in chronic ischemia or thickened in cardiomyopathy [36, 37]; *wall attenuation*, mean attenuation of the myocardial segment, which is decreased in infarction; and *systolic percentage wall thickening*, which represents regional percentage of wall thickening during systole (Ws-Wd/Wd × 100%). Normal wall thickening is 5 mm. Wall thickening is decreased in coronary artery stenosis, particularly with stress imaging due to regional hypoperfusion. In ischemic heart disease, wall motion may be difficult to evaluate, and wall thickening percentage is more accurate [11]: *wall motion* or *shortening*, displacement of points on the endocardial contour from ED to ES phase using displacement lines called chords, either in the longitudinal or circumferential plane. The length of each chord represents the amount of endocardial displacement; and *regional/segmental EF*, which represents the EF relative to a specific myocardial region/segment, is calculated by dividing ESV and EDV for a specific area beneath a myocardial segment or region [11]. Due to high variability of quantitative regional indices, qualitative or semiquantitative metrics are used, with graphics, color polar maps, and diagrams (Fig. 35.5).

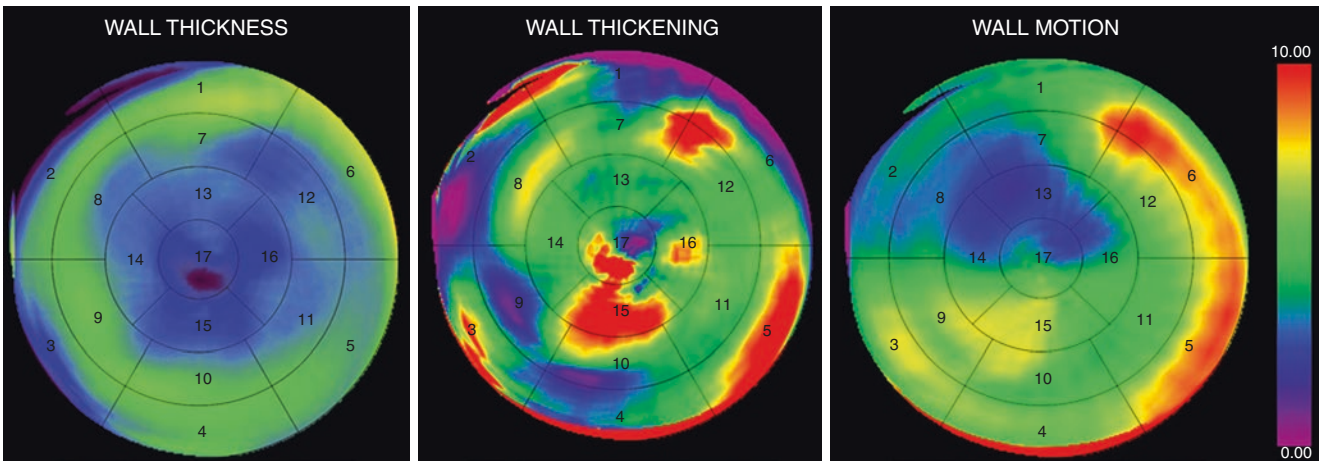

Fig. 35.5 Quantification of regional function. Polar maps showing values of myocardial wall thickness, myocardial wall thickening, and myocardial wall motion across the 17 myocardial segments as per AHA classification scheme

Diastolic Function

Diastolic dysfunction is an important factor providing diagnostic, therapeutic, and prognostic information in several disorders including CAD. This is typically performed with echocardiography. CT-derived transmitral velocity, mitral septal tissue velocity, and estimation of LV filling pressures have shown good correlation with echocardiogram [38] with comparable assessment of diastolic dysfunction; but this is not widely used clinically.

Left Ventricle

Normal functional values for the left ventricle are shown in Table 35.1 [36, 37, 39, 40]. Earlier studies showed overestimation of ESV and underestimation of EF in CT compared to CMR due to poorer temporal resolution of the earlier scanners [41, 42]. Several newer studies have shown excellent correlation between CT and CMR values, with single- and dual-source scanners of several detector widths, both at single- and multi-segment reconstruction [33, 43, 44]. Other studies have shown good correlation with and even superior accuracy than cineventriculography and transthoracic echocardiography [45, 46]. Interobserver variability of CT quantification ranges from 2% to 11% for LV EDV, 6% to 9% for ESV [11], and 2% to 8.5% for EF [3]. Most studies have also shown good sensitivity and accuracy of regional LV function assessment with CT compared to CMR, echocardiography, SPECT, and CVG [3].

Global systolic dysfunction is seen in several cardiomyopathies, both ischemic and nonischemic. Heart failure can present with either reduced or preserved ejection fractions. Hyperdynamic systolic function is seen in hypertrophic cardiomyopathies. LV function is important in the diagnosis, management, and prognosis of patients with ischemic heart disease, heart failure, malignant ventricular arrhythmia, chronic valvular regurgitation, type 2 diabetes mellitus, and congenital heart diseases [3].

Table 35.1 Normal regional LV functional parameters adapted from CMR data

	Men	Women
EDWT (mm)	7.6 ± 1.4	6.3 ± 1.0
ESWT (mm)	13.2 ± 1.8	12.2 ± 1.6
SWT (mm)	5.5 ± 0.8	5.8 ± 1.2
SWTH (%)	75 ± 16	96 ± 24

Data from Refs. [36, 37]
EDWT end-diastolic wall thickness, *ESWT* end-systolic wall thickness, *SWT* segmental wall thickening, *SWTH* segmental wall thickening percentage

Ischemic Heart Disease

LV dysfunction indicates CAD in symptomatic patients, although it is not highly sensitive. Contraction remains normal till a particular threshold for coronary blood flow is reached, below which there is an exponential fall in LV function. Dysfunction is also not specific and can happen in nonischemic cardiomyopathy, valvular heart disease, and other disorders. Wall motion abnormalities can be seen due to myocardial ischemia, hibernating myocardium, stunned myocardium, or infarct, with the last entity being irreversible. In myocardial ischemia, regional wall motion abnormalities are seen in the early stages of the disease. In acute myocardial infarction, akinesia is seen due to stunned myocardium, which may improve with revascularization [47]. Hibernating myocardium also shows functional abnormality, which improves with revascularization. CT has 89% sensitivity and 92% specificity in diagnosing abnormal segments using CMR as gold standard [48]. In patients with acute coronary syndrome (ACS) with negative troponin and EKG, coronary CTA alone has a 77% accuracy and 35% positive predictive value for detection of coronary stenosis, whereas adding functional CT improves accuracy to 87% and PPV to 80% [49] and also providing incremental value [50]. Wall motion abnormalities also highlight subtle coronary artery abnormalities that are not always evident on coronary CTA. In chronic infarct, regional wall motion abnormality such as akinesis or dyskinesis is seen with thinned myocardium in a vascular territory. Fat metaplasia, calcification, aneurysm, or pseudoaneurysm may be seen. Low EF predicts heart failure in patients with uncomplicated MI [51]. ESV is an additional independent prognostic factor in patients with previous MI and EF <40% [52]. Worsening LV EF and larger LV volumes predicted mortality in patients with CAD in the CONFIRM registry [53]. In the CASS registry, low EF was a better predictor of mortality than the number of vessels involved [2].

Heart Failure

Heart failure can be with preserved (HFpEF) or reduced ejection fraction (HFrEF). In restrictive cardiomyopathies such as amyloidosis, sarcoidosis, hemochromatosis, and glycogen storage disorders, the global systolic function is normal, but there is impaired diastolic relaxation. There is a direct correlation between LV EF and adverse outcomes including mortality. This relationship is not linear, but there is a cutoff, such as 45%, below which there is a linear relationship [2]. Nonischemic cardiomyopathies can be dilated, restrictive, hypertrophic cardiomyopathies, arrhythmogenic right ventricular dysplasia (ARVD), and unclassified disease. Most of these disorders have global systolic dysfunc-

tion, with regional wall motion abnormalities rarely seen, such as in myocarditis, sarcoidosis, and stress-induced cardiomyopathy. In dilated cardiomyopathy, the LV is dilated with global systolic dysfunction. Hypertrophic cardiomyopathy is characterized by LV thickening of several types and hyperdynamic global systolic function, with global systolic dysfunction seen in late phases of the disease. In stress-induced cardiomyopathy (Takotsubo cardiomyopathy), there is reversible global systolic dysfunction and hypokinesis/akinesis of the apical segments associated with normal contraction of the basal segments in a nonvascular distribution, which resembles a Japanese octopus pot. In reverse Takotsubo cardiomyopathy, there is hypokinesis/akinesis of the basal segments and normal contraction of apical segment. A common scenario is that in a patient with new onset heart failure and low to intermediate probability, CTA is used to exclude CAD, which can also provide functional information in the same study [10]. Similarly, in patients being evaluated for CRT, CT can provide functional information as well as venous anatomy in one study [20]. Intraventricular dysynchrony can also be evaluated to predict response to CRT [20]. Ventricular function is also accurately measured in CT in patients with cardiac transplants [54, 55] who are surviving longer, with 30% survival at 15 years [56]. In patients with left ventricular assist device (LVAD) for heart failure, CT provides accurate biventricular functional values, as well as comprehensive assessment of the device and its complications, such as location, angulation, thrombus, infection, fluid collections, pericardial effusion, and diaphragmatic hernia [57].

Right Ventricle

Right ventricle volumes and function can be qualitatively and quantitatively evaluated using retrospective ECG-gated data obtained from triphasic contrast injection protocol that opacifies both the ventricles simultaneously. Manual, automated, or semiautomated techniques can be used for quantifying volumes and function (Fig. 35.6), after determining the tricuspid annular plane. Normal values for the right ventricle in CT are shown in Table 35.2 [39]. Echocardiography is limited in the evaluation of RV due to its location behind the sternum which limits the acoustic window, complex shape which is exaggerated in abnormalities, heavy trabeculations, and thin wall [20]. CMR is considered the gold standard in the evaluation and quantification of RV [58]. However, CT is the ideal modality in the evaluation of patients who have contraindications to

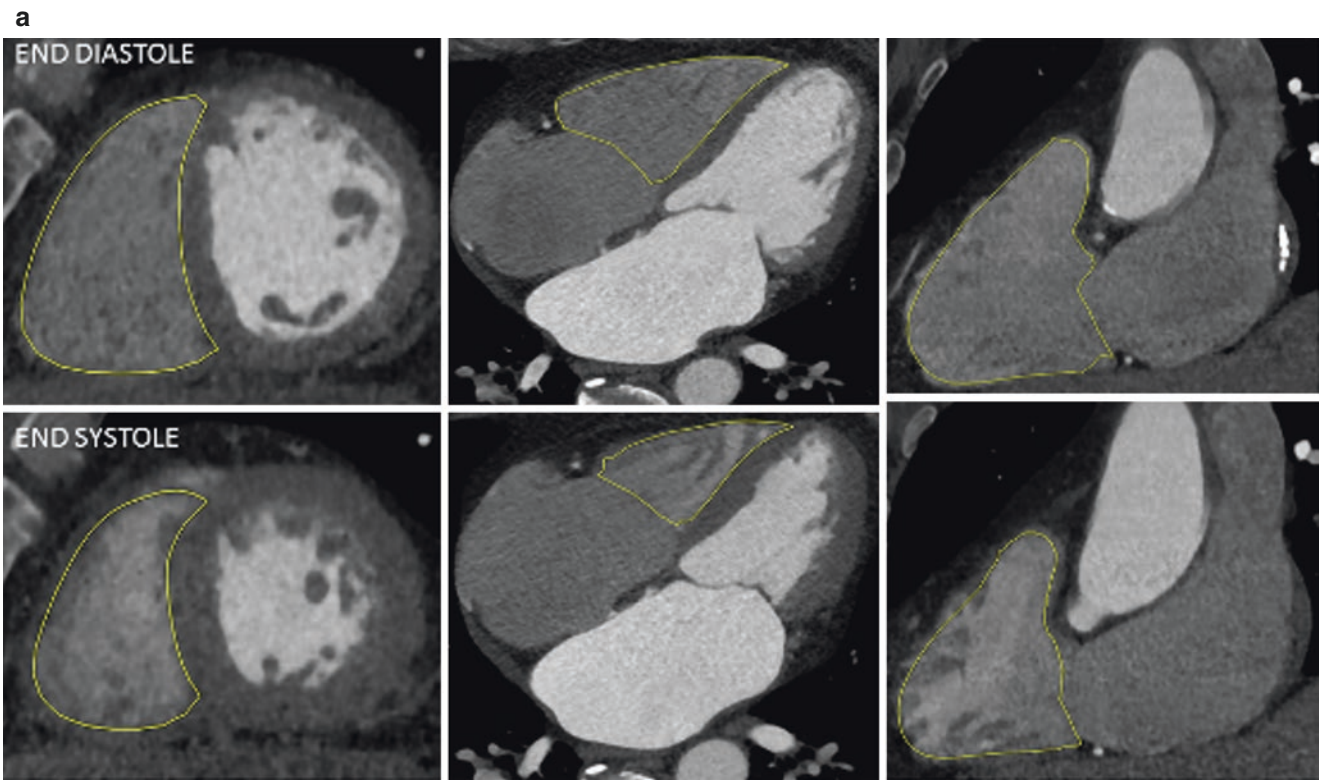

Fig. 35.6 Quantification of the right ventricle. (**a**) Short-axis (left), two-chamber (middle), and four-chamber (right) reconstructions of the heart at end-diastole (top row) and end-systole (bottom row). Endocardial (red) and epicardial (green) contours are drawn in the right ventricle both in end-diastolic and end-systolic images. (**b**) Values obtained from the above contours include ejection fraction, end-diastolic volume, end-systolic volume, stroke volume, cardiac output, and myocardial mass. All these can be indexed to the body surface area (BSA)

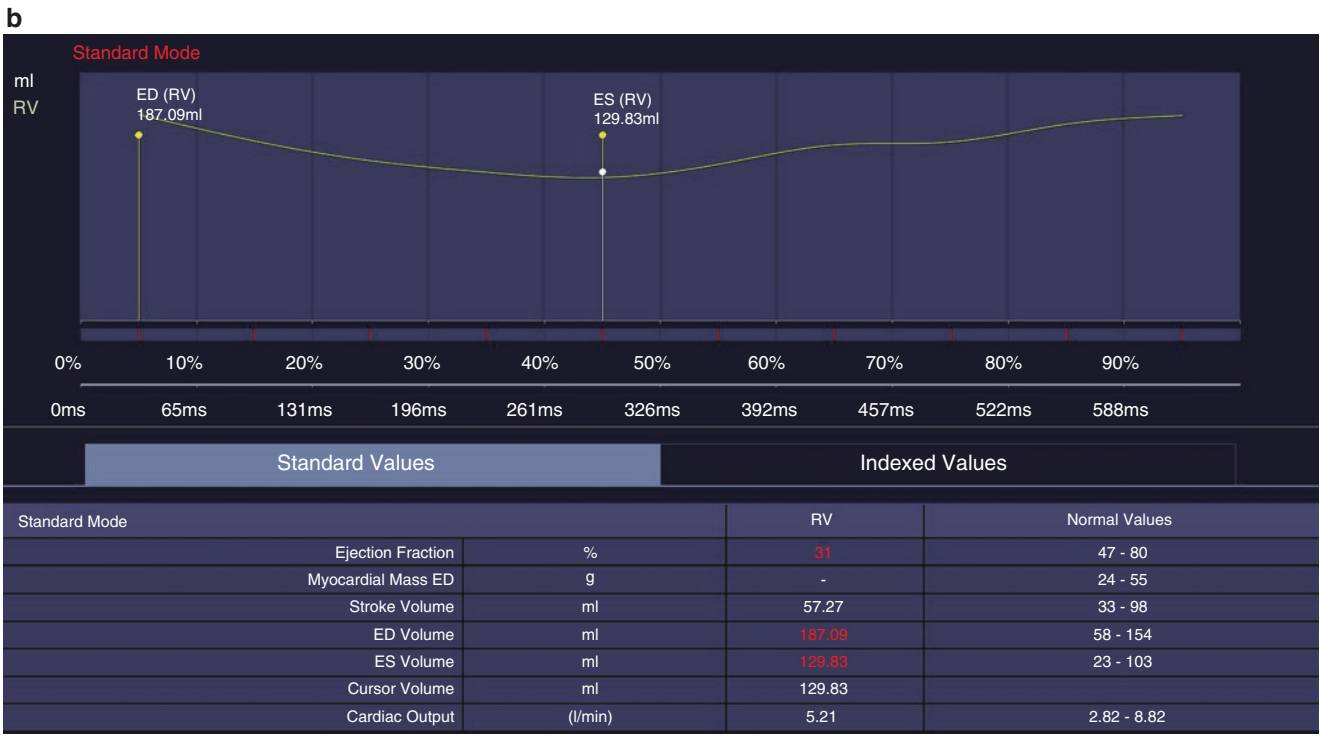

Fig. 35.6 (continued)

Table 35.2 Normal right ventricular values

ESD (mm)	29.6 ± 5.3
EDD (mm)	37.0 ± 5.7
EDV (ml)	174.9 ± 48.0
ESV (ml)	82.1 ± 29.2
EF (%)	57.9 ± 8.0

Adapted from Lin et al. [39], with permission

CMR or when artifacts are expected. Several studies have shown the high accuracy and reproducibility of CT compared to MRI in evaluation of RV function and volumes [59, 60].

RV function is an important parameter in the diagnosis, management, and prognosis of several disorders such as pulmonary embolism (PE), pulmonary hypertension, ARVD, and congenital heart disorders. In acute PE, RV dysfunction is seen when there is >30–40% of pulmonary arterial tree obstruction that has been shown to be an independent and powerful determinant of adverse prognosis [61], with higher ICU admission and death within 30 days [11]. Early identification of these high-risk patients will help in guiding them to catheter-directed thrombolysis or surgical embolectomy to reduce recurrence and death. Although ECG-gated CT is ideal for quantification of RV volumes, in the setting of acute PE, ECG gating is not always available and also not necessary. The regular axial plane or a four-chamber reconstruction can be used, and a RV/LV ratio >0.9 indicates elevated RV volume and RV strain [62] (Fig. 35.7a). Other secondary signs of RV strain include septal straightening or bowing (Fig. 35.7b), which is seen throughout cardiac cycle due to pressure overload and only in diastole for volume overload; dilated SVC (>25 mm), coronary sinus (>16 mm), and azygos vein (>25 mm); and reflux of contrast into IVC and hepatic veins [63] (Fig. 35.7c). CT can be utilized for serial changes in RV function and volumes, particularly with therapy and in those patients with contraindications for CMR (Fig. 35.8). RV dysfunction is an adverse prognostic determinant in other pulmonary disorders including cor pulmonale, interstitial lung diseases, obstructive sleep disorders, and pulmonary hypertension. For example, increased RVEDV and decreased EF have been associated with lower survival in cor pulmonale [64]. Higher RV volumes have been observed in liver diseases due to hepatopulmonary syndrome, portopulmonary hypertension, and TIPS therapy [65].

Congenital disorders including tetralogy of Fallot, transposition of great arteries, double outlet right ventricle, single ventricle physiologies, and shunt lesions (ASD, VSD, PDA, anomalous pulmonary venous return) may be associated with RV dilation and dysfunction [11]. For example, RV hypertrophy/dilation and dysfunction are seen in D-TGA following atrial switch procedure or in L-TGA due to inability of the morphologic right ventricle ("systemic ventricle")

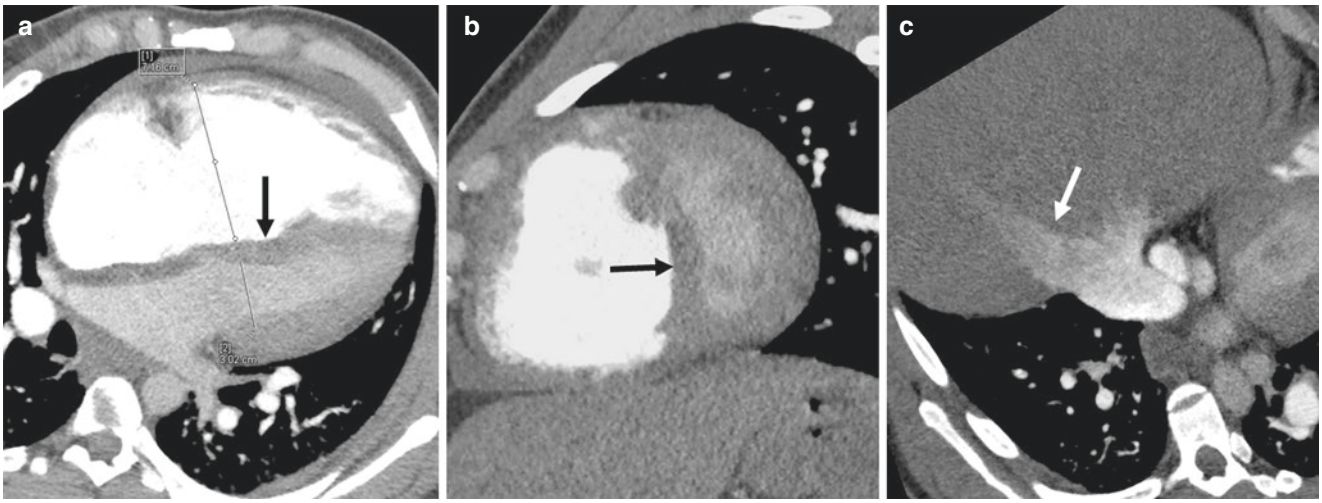

Fig. 35.7 Features of RV dysfunction in CT. (**a**) Axial CT scan shows RV/LV diameter ratio of 2.4. (**b**) Short-axis reconstruction of CT shows dilated RV and bowing of the interventricular septum (arrow) toward the LV. (**c**) Reflux of contrast in hepatic veins and IVC (arrow)

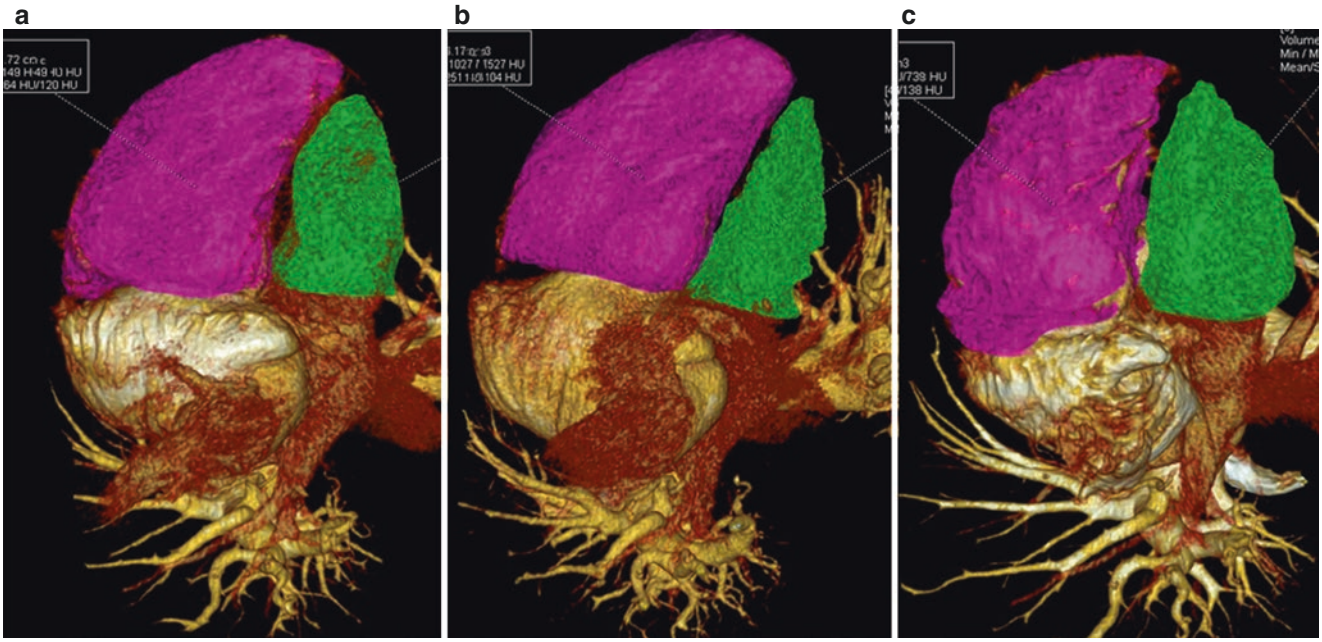

Fig. 35.8 Serial changes of RV volumes. 3D volume-rendered images in a patient with pulmonary hypertension show changes in RV volumes with time, with RVV/LVV values of 3.8 (**a**), 4.2 (**b**), and 2.6 (**c**) at 3 monthly intervals

to cope up with the systemic circulation. RV dysfunction and pulmonic regurgitation are common complications seen after surgical treatment of tetralogy of Fallot. RV function and volumes are important variables for repeat surgeries or interventional procedures such as percutaneous valve implantation. For example, pulmonary valve replacement is indicated in these patients when RVEDVI <170 ml/m^2 or RVDESVI <85 ml/m^2 [66] with lower cutoffs for chronic pulmonic regurgitation of 163 ml/m^2 and 80 ml/m^2, respectively [67].

Abnormal RV volumes and function are seen in several cardiomyopathies, particularly arrhythmogenic right ventricular dysplasia (ARVD). Recent task force criteria specify major criteria as a major wall motion abnormality (aneurysm, dyskinesis, dysynchrony, akinesia) along with RV dilation (EDVi >110 ml/m^2 in males, 100 ml/m^2 in females) or RV dysfunction (<40%). EDVi>100 ml/m^2 in males, 90 ml/m^2 in females, or RV dysfunction (40–45%) is considered as a minor criteria, although these criteria are derived from MRI [68]. ARVD is an appropriate indication for cardiac CT in 2010 ACCF guidelines [10]. Fatty tissue, bulging, and RV dilation help in distinguishing ARVD from tachyarrhythmia [69].

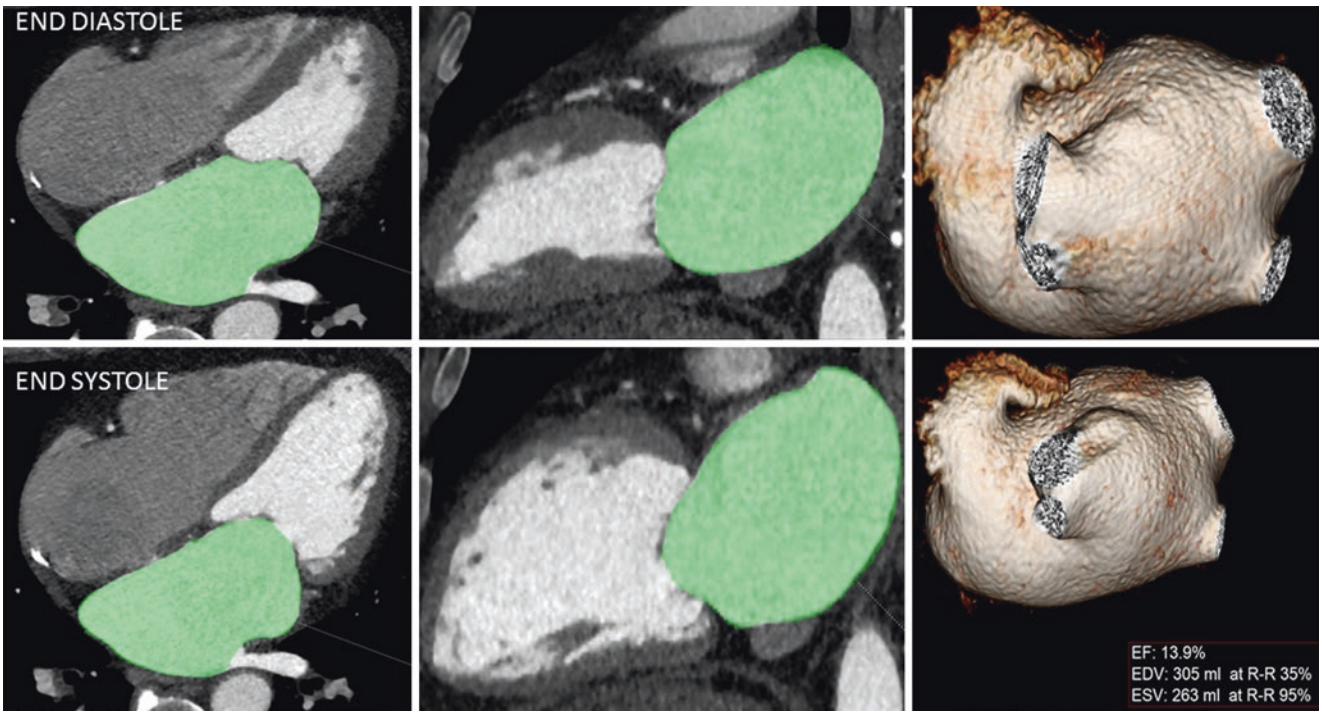

Fig. 35.9 Left atrial function. Short-axis (left), two-chamber (middle), and 3D volume-rendered (right) reconstructions of the heart at end-diastole (top row) and end-systole (bottom row). By segmenting (green) the left atrium both in end-diastole and end-systole, the left atrial volumes and function can be quantified. All these can be indexed to the body surface area (BSA)

Left Atrium

Left atrial volumes and function can be obtained from the same image data that is utilized for LV and RV quantification. Manual, semiautomated, or automated techniques are used to draw endocardial contours in the ED and ES phases with Simpson's method or used in threshold-based segmentation (Fig. 35.9).

Normal atrial filling has three phases, with an early rapid filling accounting for 75–80%, followed by diastasis accounting for 5%, and then an atrial systole accounting for 15–25% of LV blood volume [70]. Impaired relaxation of LV, with increased LA volume and lower LA EF, is seen in patients with restrictive cardiomyopathies (heart failure with preserved ejection fraction), and this can be used to distinguish it from other causes of LV hypertrophy including hypertension [71]. Although echocardiography is the most commonly used modality for evaluation of LA function, it has several limitations as discussed above. Body habitus and poor lateral resolution make it difficult to delineate the endocardium accurately in the posteriorly located left atrium, which results in lower atrial volumes and low accuracy and reproducibility [72–75]. CT values correlate with those of CMR, but usually, the LA volume is overestimated, and LA EF is underestimated [76].

Conclusion

CT provides accurate and reliable quantification of ventricular and atrial volumes and function, comparable to MRI and echocardiography. CT is used in specific circumstances where echocardiography is inadequate and MRI cannot be performed due to contraindications or artifacts. Retrospective ECG-gated spiral acquisitions are required for functional evaluation in CT, with the radiation dose minimized by using ECG-based tube current modulation.

References

1. Hammermeister KE, DeRouen TA, Dodge HT. Variables predictive of survival in patients with coronary disease. Selection by univariate and multivariate analyses from the clinical, electrocardiographic, exercise, arteriographic, and quantitative angiographic evaluations. Circulation. 1979;59(3):421–30.
2. Mock MB, Ringquist I, Fisher LD, et al. Survival of medically treated patients in the coronary artery surgery study (CASS) registry. Circulation. 1982;66:562–8.
3. Sayyed SH, Cassidy MM, Hadi MA. Use of multidetector computed tomography for evaluation of global and regional left ventricular function. J Cardiovasc Comput Tomogr. 2009;3(S1):S23–34.
4. Setser RM, Eischer SE, Lorenz CH. Quantification of left ventricular function with magnetic resonance images acquired in real time. J Magn Reson Imaging. 2000;12:430–8.

5. de Geus-Oei LF, Mavinkurve-Groothuis AM, Bellerson L, et al. Scintigraphic techniques for early detection of cancer treatment-induced cardiotoxicity. J Nucl Med. 2011;52(4):560–71.
6. Slart RH, Bax JJ, de Jong RM, et al. Comparison of gated PET with MRI for evaluation of left ventricular function in patients with coronary artery disease. J Nucl Med. 2004;45(2):176–82.
7. Bavelaar-Croon CD, Kayser HW, van der Wall EE, et al. Left ventricular function: correlation of quantitative gated SPECT and MR imaging over a wide range of values. Radiology. 2000;217(2):572–5.
8. Bodenheimer MMBV, Fooshee CM, Hermann GA, et al. Comparison of wall motion and regional ejection fraction at rest and during isometric exercise: concise communication. J Nucl Med. 1979;20:724–32.
9. Stollfuss JC, Haas F, Matsunari I, et al. Regional myocardial wall thickening and global ejection fraction in patients with low angiographic left ventricular ejection fraction assessed by visual and quantitative resting ECG-gated 99mTc-tetrofosmin single-photon emission tomography and magnetic resonance imaging. Eur J Nucl Med. 1998;25(5):522–30.
10. Taylor AJ, Cerqueira M, Hodgson JM, et al. ACCF/SCCT/ACR/AHA/ASE/ASNC/SCAI/SCMR 2010 appropriate use criteria for cardiac computed tomography. J Am Coll Cardiol. 2010;56(22):1864–94.
11. Savino G, Zwerner P, Herzog C, et al. CT of cardiac function. J Thorac Imaging. 2007;22:86–100.
12. Ritchie C, Godwin J, Crawford C, et al. Minimum scan speeds for suppression of motion artifacts in CT. Radiology. 1992;185:37–42.
13. Port S, Cobb FR, Jones RH. Effects of propranolol on left ventricular function in normal men. Circulation. 1989;61(12):358–66.
14. Mo YH, Jaw FS, Wang YC, et al. Effects of propranolol on the left ventricular volume of normal subjects during CT coronary angiography. Korean J Radiol. 2011;12(3):319.
15. Dell'Italia LJ, Walsh RA. Effect of intravenous metoprolol on left ventricular performance in Q-wave acute myocardial infarction. Am J Cardiol. 1989;63(3):166–71.
16. Jensen CJ, Jochims M, Hunold P, et al. Assessment of left ventricular function and mass in dual-source computed tomography coronary angiography: influence of beta-blockers on left ventricular function: comparison to magnetic resonance imaging. Eur J Radiol. 2010;74(3):484–91.
17. Lee H, Kim SY, Gebregziabher M, et al. Impact of ventricular contrast medium attenuation on the accuracy of left and right ventricular function analysis at cardiac multi detector-row CT compared with cardiac MRI. Acad Radiol. 2012;19(4):395–405.
18. Gao Y, Du X, Liang L, et al. Evaluation of right ventricular function by 64-row CT in patients with chronic obstructive pulmonary disease and cor pulmonale. Eur J Radiol. 2012;81(2):345–53.
19. Cademartiri F, Nieman K, van der Lugt A, et al. Intravenous contrast material administration at 16-detector row helical CT coronary angiography: test bolus versus bolus-tracking technique. Radiology. 2004;233(3):817–23.
20. Rizvi A, Deano RC, Bachman DP, et al. Analysis of ventricular function by computed tomography. J Cardiovasc Comput Tomogr. 2015;9(1):1–12.
21. Takx RAP, Moscariello A, Schoepf UJ, et al. Quantification of left and right ventricular function and myocardial mass: comparison of low-radiation dose 2nd generation dual-source CT and cardiac MRI. Eur J Radiol. 2012;81(4):e598–604.
22. Hausleiter J, Meyer T, Hadamitzky M, et al. Radiation dose estimates from cardiac multislice computed tomography in daily practice. Circulation. 2006;113:1305–10.
23. Hausleiter J, et al. A new algorithm for ECG-based tube current modulation ("MinDose") reduces radiation dose estimates in cardiac dual source CT angiography. Circulation. 2007;116(Suppl 16):II-575.
24. Feuchtner G, Goetti R, Plass A, et al. Dual-step prospective ECG-triggered 128-slice dual source CT for evaluation of coronary arteries and cardiac function without heart rate control a technical note. Eur Radiol. 2010;20:2092–9.
25. Ko YJ, Kim SS, Park WJ, et al. Comparison of global left ventricular function using 20 phases with 10-phase reconstructions in multidetector-row computed tomography. Int J Cardiovasc Imaging. 2012;28(3):603–11.
26. Puesken M, Fischbach R, Wenker M, et al. Global left-ventricular function assessment using dual-source multidetector CT: effect of improved temporal resolution on ventricular volume measurement. Eur Radiol. 2008;18(10):2087–94.
27. Wai B, Thai WE, Brown H, et al. Novel phase-based noise reduction strategy for quantification of left ventricular function and mass assessment by cardiac CT: comparison with cardiac magnetic resonance. Eur J Radiol. 2013;82:e337–41.
28. Lessick J, Ghersin E, Abadi S, Yalonetsky S. Accuracy of the long-axis area-length method for the measurement of left ventricular volumes and ejection fraction using multidetector computed tomograph. Can J Cardiol. 2008;24(9):685–9.
29. Greupner J, Zimmermann E, Hamm B, Dewey M. Automatic versus semiautomatic global cardiac function assessment using 64-row computed tomography. Br J Radiol. 2012;85(1015):e243–53.
30. Juergens KU, Seifarth H, Range F, et al. Automated threshold-based 3D segmentation versus short-axis planimetry for assessment of global left ventricular function with dual-source MDCT. Am J Roentgenol. 2008;190(2):308–14.
31. Plumhans C, Keil S, Ocklenburg C, et al. Comparison of manual, semi- and fully automated heart segmentation for assessing global left ventricular function in multidetector computed tomography. Investig Radiol. 2009;44(8):476–82.
32. van Ooijen PM, de Jonge GJ, Oudkerk M. Informatics in radiology: Postprocessing pitfalls in using CT for automatic and semiautomatic determination of global left ventricular function. Radiographics. 2012;32(2):589–99.
33. de Jonge GJ, can der Vleuten PA, Overbosch J, et al. Semiautomatic measurement of left ventricular function on dual source computed tomography using five different software tools in comparison with magnetic resonance imaging. Eur J Radiol. 2011;80(3):755–66.
34. Mao SS, Li D, Rosenthal DG, et al. Dual-standard reference values of left ventricular volumetric parameters by multidetector CT angiography. J Cardiovasc Comput Tomogr. 2013;7:234–40.
35. Juergens UK, Fischbach R. Left ventricular function studied with MDCT. Eur Radiol. 2006;16:342–57.
36. Alfakih K, Plein S, Thiele H, et al. Normal human left and right ventricular dimensions for MRI as assessed by turbo gradient echo and steady state free precession imaging sequences. J Magn Reson Imaging. 2003;17:323–9.
37. Sandstede J, Lipke C, Beer M, et al. Age and gender specific differences in left and right ventricular cardiac function and mass determined by cine magnetic resonance imaging. Eur Radiol. 2000;10:438–42.
38. Boogers MJ, van Werkhoven JM, Shuijf JD, et al. Feasibility of diastolic functional assessment with cardiac CT: feasibility study in comparison with tissue Doppler imaging. JACC Cardiovasc Imaging. 2011;4:246–56.
39. Lin FY, et al. Cardiac chamber volumes, function, and mass as determined by 64-multidetector row computed tomography: mean values among healthy adults free of hypertension and obesity. JACC Cardiovasc Imaging. 2008;1(6):782–6.
40. Nevsky G, Jacobs JE, Lim RP, et al. Sex-specific normalized reference values of heart and great vessel dimensions in cardiac CT angiography. Am J Roentgenol. 2011;196:788–94.
41. Juergens KU, Grude M, Maintz D, et al. Multi-detector row CT of left ventricular function with dedicated analysis software versus MR imaging: initial experience. Radiology. 2004;230:403–10.

42. Mahnken AH, Speuntrup E, Neithammer M, et al. Quantitative and qualitative assessment of left ventricular volume with ECG-gated multislice spiral CT: value of different image reconstruction algorithms in comparison to MRI. Acta Radiol. 2003;44(6):604–11.
43. van der Vleuten PA, Willems TP, Gotte MJ, et al. Quantification of global left ventricular function: comparison of multidetector computed tomography and magnetic resonance imaging. A meta-analysis and review of the current literature. Acta Radiol. 2006;47(10):1049–57.
44. Grude M, Juegens KU, Wichter T, et al. Evaluation of global left ventricular myocardial function with electrocardiogram gated multidetector computed tomography. Comparison with magnetic resonance imaging. Investig Radiol. 2003;38:653–61.
45. Asferg C, Usinger L, Kristensen TS, et al. Accuracy of multi-slice computed tomography for measurement of left ventricular ejection fraction compared with cardiac magnetic resonance imaging and two-dimensional transthoracic echocardiography: a systematic review and metaanalysis. Eur J Radiol. 2011;81:e756–62.
46. Dewey M, Muller M, Eddicks S, et al. Evaluation of global and regional left ventricular function with 16-slice computed tomography, biplane cineventriculography and two-dimensional transthoracic echocardiography: comparison with magnetic resonance imaging. J Am Coll Cardiol. 2006;48:2034.
47. Mahias-Narvarte AHKF, Willis PW. Evolution of regional left ventricular wall motion abnormalities in acute Q and non-Q wave myocardial infarction. American Heart Journal. 1987;113:1369–75.
48. Sarwar A, Shapiro MD, Nasir K, et al. Evaluating global and regional left ventricular function in patients with reperfused acute myocardial infarction by 64-slice multidetector CT: a comparison to magnetic resonance imaging. J Cardiovasc Comput Tomogr. 2009;3(3):170–7.
49. Seneviratne SK, Troung QA, Bamberg F, et al. Incremental diagnostic value of regional left ventricular function over coronary assessment by cardiac computed tomography for the detection of acute coronary syndrome in patients with acute chest pain: from the ROMICAT trial. Circ Cardiovasc Imaging. 2010;3(8):375–83.
50. Bezerra HG, Loureiro R, Irlbeck T, et al. Incremental value of myocardial perfusion over regional left ventricular function and coronary stenosis by cardiac CT for detection of acute coronary syndromes in high risk patients: a subgroup analysis of the ROMICAT trial. J Cardiovasc Comput Tomogr. 2011;5:382–91.
51. Candell-Riera JLJ, Santana C, Castell J, et al. Prognostic assessment of uncomplicated first myocardial infarction by exercise echocardiography and Tc-99m tetrofosmin gated SPECT. J Nucl Cardiol. 2001;81:122–8.
52. Antonini-Canterin FNG. Valutazione eoardiografica dei volume e della funzione sistolica globale del ventricolo sinistro. Ital Heart J. 2000;1:1261–72.
53. Arsanjani R, Berman DS, Gransar H, et al. Left ventricular function and volume with coronary CT angiography improves risk stratification and identification of patients at risk for incident mortality: results from 7758 patients in the prospective multinational CONFIRM observational cohort study. Radiology. 2014;273(1):70–7
54. Mastrobuoni S, Dell'aquila AM, Arraiza M, et al. Allograft morphology and function in heart transplant recipients surviving more than 15 years by magnetic resonance imaging and dual-source computed tomography. Eur J Cardiothorac Surg. 2011;40(1):e62–6.
55. Bastarrika G, Arraiza M, DeCecco CN, et al. Quantification of left ventricular function and mass in heart transplant recipients using dual-source CT and MRI: initial clinical experience. Eur Radiol. 2008;18(9):1784–90.
56. Taylor DO, Edwards LB, Aurora P, et al. Registry of the International Society for Heart and Lung Transplantation: twenty-fifth official adult heart transplant report—2008. J Heart Lung Transplant. 2008;27(9):943–56.
57. Acharya D, Singh S, Tallaj JA, et al. Use of gated cardiac computed tomography angiography in the assessment of left ventricular assist device dysfunction. ASAIO J. 2011;57:32–7.
58. Geva T. Is MRI the preferred method for evaluating right ventricular size and function in patients with congenital heart disease? Circ Cardiovasc Imaging. 2014;7:190–7.
59. Raman SV, Shah M, McCarthy B, et al. Multi-detector row cardiac computed tomography accurately quantifies right and left ventricular size and function compared with cardiac magnetic resonance. Am Heart J. 2006;151:736–44.
60. Guo YK, Gao HL, Zhang XC, et al. Accuracy and reproducibility of assessing right ventricular function with 64-section multidetector row CT: comparison with magnetic resonance imaging. Int J Cardiol. 2010;139:254–62.
61. Kang DK, Thilo C, Schoepf UJ, et al. CT signs of right ventricular dysfunction. J Am Coll Cardiol Img. 2011;4(8):841–9.
62. Quiroz R, Kucher N, Schoepf UJ, et al. Right ventricular enlargement on chest computed tomography: prognostic role in acute pulmonary embolism. Circulation. 2004;109(20):2401–4.
63. Staskiewicz G, Czekajska-Chehab E, Przegalinski J, et al. Widening of coronary sinus in CT pulmonary angiography indicates right ventricular dysfunction in patients with acute pulmonary embolism. Eur Radiol. 2010;20:1615–20.
64. Burgess MI, Mogulkoc N, Bright-Thomas RJ, et al. Comparison of echocardiographic markers of right ventricular function in determining prognosis in chronic pulmonary disease. J Am Soc Echocardiogr. 2002;15:633–9.
65. Dupont MVM, Dragean CA, Coche EE. Right ventricle function assessment by MDCT. Am J Roentgenol. 2011;196(1):77–86.
66. Therrien J, Provost Y, Merchant N, et al. Optimal timing for pulmonary valve replacement in adults after tetralogy of Fallot repair. Am J Cardiol. 2005;95:779–82.
67. Lee C, Kim YM, Lee CH, et al. Outcomes of pulmonary valve replacement in 170 patients with chronic pulmonary regurgitation after relief of right ventricular outflow tract obstruction: implications for optimal timing of pulmonary valve replacement. J Am Coll Cardiol. 2012;60:1005–14.
68. Marcus F, McKenna WJ, Sherrill D, et al. Diagnosis of arrhythmogenic right ventricular cardiomyopathy/dysplasia: proposed modification of the task force criteria. Eur Heart J. 2010;31(7):806–14.
69. Nakajima T, Kimura F, Kajimoto K, et al. Utility of ECG-gated MDCT to differentiate patients with ARVC/D from patients with ventricular tachyarrhythmias. J Cardiovasc Comput Tomogr. 2013;7:223–33.
70. Stojanovska J, Cronin P, Patel S, et al. Reference normal absolute and indexed values from ECG-gated MDCT: left atrial volume, function, and diameter. Am J Roentgenol. 2011;197(3):631–7.
71. Melenovsky V, Borlaug B, Rosen, et al. Cardiovascular features of heart failure with preserved ejection fraction versus non-failing hypertensive left ventricular hypertrophy in the urban Baltimore community. J Am Coll Cardiol. 2007;49:198.
72. Avelar E, Durst R, Rosito GA, et al. Comparison of the accuracy of multidetector computed tomography versus two-dimensional echocardiography to measure left atrial volume. Am J Cardiol. 2010;106(1):104–9.
73. Rodevan O, Bjornerheim R, Ljosland M, et al. Left atrial volumes assessed by three- and two-dimensional echocardiography compared to MRI estimates. Int J Card Imaging. 1999;15:397–410.
74. Christiaens L, Lequeux B, Ardilouze P, et al. A new method for measurement of LA volumes using 64-slice spiral CT: comparison with 2DE techniques. Int J Cardiol. 2009;131:217–24.
75. Kircher B, Abbott JA, Paul S, et al. Left atrial volume determination by biplane two-dimensional echocardiography: validation by cine CT. Am Heart J. 1991;121:864–71.
76. Wen Z, Zhang Z, Yu W, et al. Assessing the left atrial phase volume and function with dual-source CT: comparison with 3T MRI. Int J Cardiovasc Imaging. 2010;26:88–92.